Infectious Disease Modelling 9 (2024) 689–700

Contents lists available at ScienceDirect

Infectious Disease Modelling

journal homepage: www.keaipublishing.com/idm

Epidemiological feature analysis of SVEIR model with control strategy and variant evolution

Kaijing Chen [a], Fengying Wei [a, b, c, *], Xinyan Zhang [d, **], Hao Jin [d], Zuwen Wang [a], Yue Zuo [d], Kai Fan [d]

[a] School of Mathematics and Statistics, Fuzhou University, Fuzhou, 350116, Fujian, China
[b] Key Laboratory of Operations Research and Control of Universities in Fujian, Fuzhou University, Fuzhou, 350116, Fujian, China
[c] Center for Applied Mathematics of Fujian Province, Fuzhou University, Fuzhou, 350116, Fujian, China
[d] Jinzhou Center for Disease Control and Prevention, Jinzhou, 121000, Liaoning, China

ARTICLE INFO

Article history:
Received in revised form 26 February 2024
Accepted 22 March 2024
Handling Editor: Dr Yijun Lou

Keywords:
COVID-19
SVEIR model
Twenty measures
Control strategy
Variant evolution

ABSTRACT

The complex interactions were performed among non-pharmaceutical interventions, vaccinations, and hosts for all epidemics in mainland China during the spread of COVID-19. Specially, the small-scale epidemic in the city described by SVEIR model was less found in the current studies. The SVEIR model with control was established to analyze the dynamical and epidemiological features of two epidemics in Jinzhou City led by Omicron variants before and after Twenty Measures. In this study, the total population (N) of Jinzhou City was divided into five compartments: the susceptible (S), the vaccinated (V), the exposed (E), the infected (I), and the recovered (R). By surveillance data and the SVEIR model, three methods (maximum likelihood method, exponential growth rate method, next generation matrix method) were governed to estimate basic reproduction number, and the results showed that an increasing tendency of basic reproduction number from Omicron BA.5.2 to Omicron BA.2.12.1. Meanwhile, the effective reproduction number for two epidemics were investigated by surveillance data, and the results showed that Jinzhou wave 1 reached the peak on November 1 and was controlled 7 days later, and that Jinzhou wave 2 reached the peak on November 28 and was controlled 5 days later. Moreover, the impacts of non-pharmaceutical interventions (awareness delay, peak delay, control intensity) were discussed extensively, the variations of infection scales for Omicron variant and EG.5 variant were also discussed. Furthermore, the investigations on peaks and infection scales for two epidemics in dynamic zero-COVID policy were operated by the SVEIR model with control. The investigations on public medical requirements of Jinzhou City and Liaoning Province were analyzed by using SVEIR model without control, which provided a possible perspective on variant evolution in the future.

1. Introduction

The Chinese government promptly took the prevention and control measures to control the spread of COVID-19 within a relatively short period of time (Hellewell et al., 2020; Niu & Xu, 2020), due to the sudden outbreak of COVID-19 at the end of

* Corresponding author. School of Mathematics and Statistics, Fuzhou University, Fuzhou, 350116, Fujian, China.
** Co-corresponding author.
E-mail addresses: 747508471@qq.com (K. Chen), weifengying@fzu.edu.cn (F. Wei), pengyou88888123@126.com (X. Zhang).
Peer review under responsibility of KeAi Communications Co., Ltd.

https://doi.org/10.1016/j.idm.2024.03.005

2019. However, the evolution of variants, the mobility of population, and the importation of infection cases were main factors for the local prevalence of COVID-19 in mainland China (Guo et al., 2022; Wei, Li, et al., 2023). Although, normalization stage prevention and control, dynamic zero-COVID policy, Twenty Measures, Ten New Measures were implemented by the Chinese government against COVID-19 with the minimal losses (Liu et al., 2022; Liang et al., 2021; Lin et al., 2022; The State Council joint prevention and control mechanism against COVID-19, 2022,b). With the international situation of COVID-19, the assessment by mathematical models was one of the most effective approaches when studying an epidemic course. Specially, the SEIR models were widely applied to explore the scenario investigations and the long-term behaviors of transmission mechanism of COVID-19 (Guo et al., 2023; Guo et al., 2023; He et al., 2023; Liu et al., 2023; Shen et al., 2021; Song et al., 2022; Tang et al., 2020; Yu et al., 2023; Zhao et al., 2022; Zou et al., 2022). For instance, the impact of vaccination (Song et al., 2022; Yu et al., 2023), the impact of non-pharmacological interventions (Guo et al., 2023; Shen et al., 2021; Zhao et al., 2022; Zou et al., 2022) and the impact of variant evolution (Guo et al., 2023; He et al., 2023; Liu et al., 2023) were extensively investigated in the recent studies. However, the small-scale and short-duration epidemic was seldom focused on exploring the dynamical and epidemiological features. This study would detect the internal mechanism led by distinct variants through establishing the SVEIR model below.

2. Methods

2.1. Data sources and analysis

The surveillance data of infection cases for Jinzhou wave 1 (October 28, 2022—November 8, 2022) and Jinzhou wave 2 (November 21, 2022—December 5, 2022) were provided by Jinzhou Center for Disease Control and Prevention (i.e., Jinzhou CDC). The gender, age, symptom, street-level address and vaccination were included in this study. The majority of infection cases were mainly asymptomatic (Supplementary Table 1 and Supplementary Table 2). Moreover, the age distribution and vaccination doses for infection cases were provided in Supplementary Fig. 2.

2.2. Model with control

The previous studies included incubation period (Chen & Wei, 2020; Lan et al., 2023a,c; Wei & Xue, 2020), vaccination (Li et al., 2022; Lu & Wei, 2019; Wei, Li, et al., 2023; Xiong et al., 2024), control strategies (He et al., 2021; Li & Xiao, 2023; Lovell-Read et al., 2022) and awareness delay (Huang et al., 2020; Lan et al., 2023b; Wei, Li, et al., 2023) motivated us to establish an SVEIR model, for describing the small-scale and short-duration Jinzhou epidemics. The flow diagram of the disease transmission was shown in Fig. 1. The parameters in this figure were set as follows: β_1 denoted the infection rate between the susceptible and the infected, β_2 denoted the infection rate between the vaccinated and the infected. u denoted the intensity of control. Exposed people developed to infected people at a rate coefficient α, where $\frac{1}{\alpha}$ was the mean incubation period. γ denoted the average recovery time. In this study, we assumed that: (i) N was set to be a constant, the natural birth rate and natural death rate were neglected due to short duration of Jinzhou epidemics. (ii) The infection rate of V was much lower than that of S due to the vaccination. (iii) E were not capable of infecting others. (iv) I had the ability to infect others. (v) R were regarded to be with temporary immunities. Therefore, an SVEIR model with control was proposed to investigate dynamical and epidemiological features of Jinzhou epidemics.

$$\begin{cases} \dot{S}(t) = -\beta_1(1-u)SI, \\ \dot{V}(t) = -\beta_2 VI, \\ \dot{E}(t) = \beta_1(1-u)SI + \beta_2 VI - \alpha E, \\ \dot{I}(t) = \alpha E - \gamma I, \\ \dot{R}(t) = \gamma I. \end{cases} \tag{1}$$

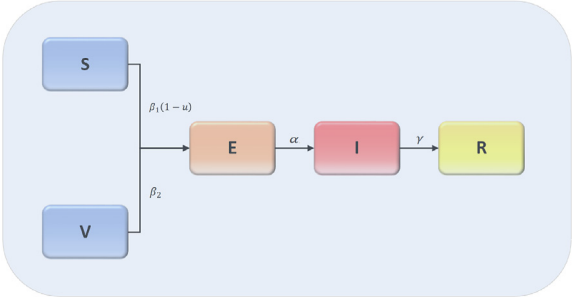

Fig. 1. Flow diagram of the disease transmission.

It was of importance to figure out the total population due to the small-scale and short-duration of two epidemics in Jinzhou City. The provided data method was referred, as the numbers of the individuals who were under control were directly provided by Jinzhou CDC. The estimated data method was referred, as using street-level infection cases, sex ratio and age group ratios in Supplementary Table 4 - Supplementary Table 6 to estimate the total population in Table 1.

2.3. Parameter estimation by Least Squares Method

The parameter estimation was crucial and important for identifying epidemiological indices and characteristics. Therefore, the Least Squares Method that allowed the minimum loss between the simulation and the surveillance data (Hamou et al., 2022) was governed for the main parameters and their estimations in Supplementary Table 3.

2.4. Estimation method for basic reproduction number

The epidemiologic definition of basic reproduction number $\mathcal{R}_0$ was the average number of secondary cases generated by an infected case who spread virus towards the susceptible (Van den Driessche, 2017). In this study, the maximum likelihood method, the exponential growth rate method, the next generation matrix method were used to perform the evaluation of basic reproduction number $\mathcal{R}_0$.

2.4.1. Maximum likelihood method

The maximum likelihood method (ML) was proposed by White and Pagano (Forsberg White and Pagano, 2008). This method required the assumptions that the population was all uniformly distributed, that there were no missing data, that there were no input cases, and that the second-generation cases were all generated obeying a poisson distribution with an expectation value of $\mathcal{R}_0$. The estimation of $\mathcal{R}_0$ was carried out by using the following formula:

$$L(\mathcal{R}_0, \boldsymbol{\omega}) = \sum_{i=1}^{T} \log \frac{e^{-\mu_t} \mu_t^{N_t}}{N_t!}, \quad \mu_t = \mathcal{R}_0 \sum_{i=1}^{t} N_{t-i}\omega_i, \tag{2}$$

here, N_t denoted the number of infection cases in a continuous time, ω_i, the generation time distribution.

2.4.2. Exponential growth rate method

The exponential growth rate method (EGR) was proposed by Wallinga and Lipsitch (Wallinga & Lipsitch, 2007). This method utilized the exponential growth rate of the number of infection cases that calculated from a poisson distribution during the initial period of the epidemic (i.e., the period that infection cases exponentially grew in the number), combined with a time distribution to calculate $\mathcal{R}_0$. The estimation of $\mathcal{R}_0$ was applied by using the following formula:

$$\mathcal{R}_0 = \frac{1}{M(-r)} = \left\{ \int_0^{\infty} e^{-rt} \omega(t) \mathrm{d}t \right\}^{-1}, \tag{3}$$

here, M denoted the moment-generation function of the generation time distribution $\omega(t)$, r for the exponential growth rate.

2.4.3. Next generation matrix method

The expression of basic reproduction number $\mathcal{R}_0$ of SVEIR model was calculated by using the next generation matrix method (Van den Driessche & Watmough, 2002), incorporating parameter estimations from Least Squares Method. As discussed in the recent studies (Chen et al., 2020; Lin et al., 2020), there were two infected compartments of the model, denoted as E and I. We could write

Table 1
Descriptions and initial values for two epidemics in Jinzhou City during dynamic zero-COVID policy.[a].

Variable	Description	Initial value				Source
		Provided data method		Estimated data method		
		Jinzhou wave 1	Jinzhou wave 2	Jinzhou wave 1	Jinzhou wave 2	
$N(0)$	Initial value of total population	11,992	47,954	82,942	184,677	Jinzhou CDC
$S(0)$	Initial value of the susceptible	2028	8126	14,058	31,307	Jinzhou CDC
$V(0)$	Initial value of the vaccinated	9958	398,21	68,878	153,363	Jinzhou CDC
$E(0)$	Initial value of the exposed	6	7	6	7	Jinzhou CDC
$I(0)$	Initial value of the infected	0	0	0	0	Jinzhou CDC
$R(0)$	Initial value of the recovered	0	0	0	0	Jinzhou CDC

[a] If the NPIs were not performed, then, the total population of Jinzhou City was $N(0) = 2, 703, 853$ (Jinzhou Bureau of Statistics, 2021), the number of the exposed for Jinzhou wave 1 was set to be $E(0) = 395$, the number of the exposed for Jinzhou wave 2 was set to be $E(0) = 395$.

$$\begin{aligned}\dot{E}(t) &= \mathcal{F}_1(S(t),V(t),E(t),I(t)) - \mathcal{V}_1(S(t),V(t),E(t),I(t)) \\ &= (\beta_1(1-u)SI + \beta_2 VI) - (\alpha E),\end{aligned}$$

$$\begin{aligned}\dot{I}(t) &= \mathcal{F}_2(S(t),V(t),E(t),I(t)) - \mathcal{V}_2(S(t),V(t),E(t),I(t)) \\ &= 0 - (-\alpha E + \gamma I).\end{aligned}$$

Thus, we obtained

$$F = \begin{pmatrix} \frac{\partial \mathcal{F}_1}{\partial E} & \frac{\partial \mathcal{F}_1}{\partial I} \\ \frac{\partial \mathcal{F}_2}{\partial E} & \frac{\partial \mathcal{F}_2}{\partial I} \end{pmatrix} = \begin{pmatrix} 0 & \beta_1(1-u)S_0 + \beta_2 V_0 \\ 0 & 0 \end{pmatrix}, \tag{4}$$

$$V = \begin{pmatrix} \frac{\partial \mathcal{V}_1}{\partial E} & \frac{\partial \mathcal{V}_1}{\partial I} \\ \frac{\partial \mathcal{V}_2}{\partial E} & \frac{\partial \mathcal{V}_2}{\partial I} \end{pmatrix} = \begin{pmatrix} \alpha & 0 \\ -\alpha & \gamma \end{pmatrix}, \tag{5}$$

which gave

$$V^{-1} = \begin{pmatrix} \frac{1}{\alpha} & 0 \\ \frac{1}{\gamma} & \frac{1}{\gamma} \end{pmatrix}.$$

The next generation matrix was defined as $M = FV^{-1}$, that was

$$M = \begin{pmatrix} \frac{\beta_1(1-u)S_0 + \beta_2 V_0}{\gamma} & \frac{\beta_1(1-u)S_0 + \beta_2 V_0}{\gamma} \\ 0 & 0 \end{pmatrix}. \tag{6}$$

Since the spectral radius of M-matrix was defined as the basic reproduction number $\mathcal{R}_0$, we obtained the specific expression of $\mathcal{R}_0$

$$\mathcal{R}_0 = \frac{\beta_1(1-u)S_0 + \beta_2 V_0}{\gamma} \tag{7}$$

with

$$\beta_1 = \frac{\beta_1^1 \times d_1 + \beta_1^2 \times d_2}{d_1 + d_2}. \tag{8}$$

Here, d_1 denoted the days spent before control; d_2, the days spent after control; β_1^1, the infection rates before control; β_1^2, the infection rates after control; β_1^a, the average infection rates in $d_1 + d_2$ days. S_0 and V_0 were the initial values of the local population.

2.5. Effective reproduction number

The effective reproduction number $\mathcal{R}_t$ provided the transmission tendency of an epidemic course, and was defined as the average number of secondary cases caused by the primary case at time t (Chowell & Nishiura, 2009). When $\mathcal{R}_t$ was less than 1, the epidemic was regarded as under effective control. Otherwise, the epidemic was prevalent. The surveillance data of two epidemics in Jinzhou City were collected before and after the implementation of Twenty Measures for providing the curves of $\mathcal{R}_t$ in Fig. 3 by the EpiEstim R package (Cori et al., 2013) and matlab.

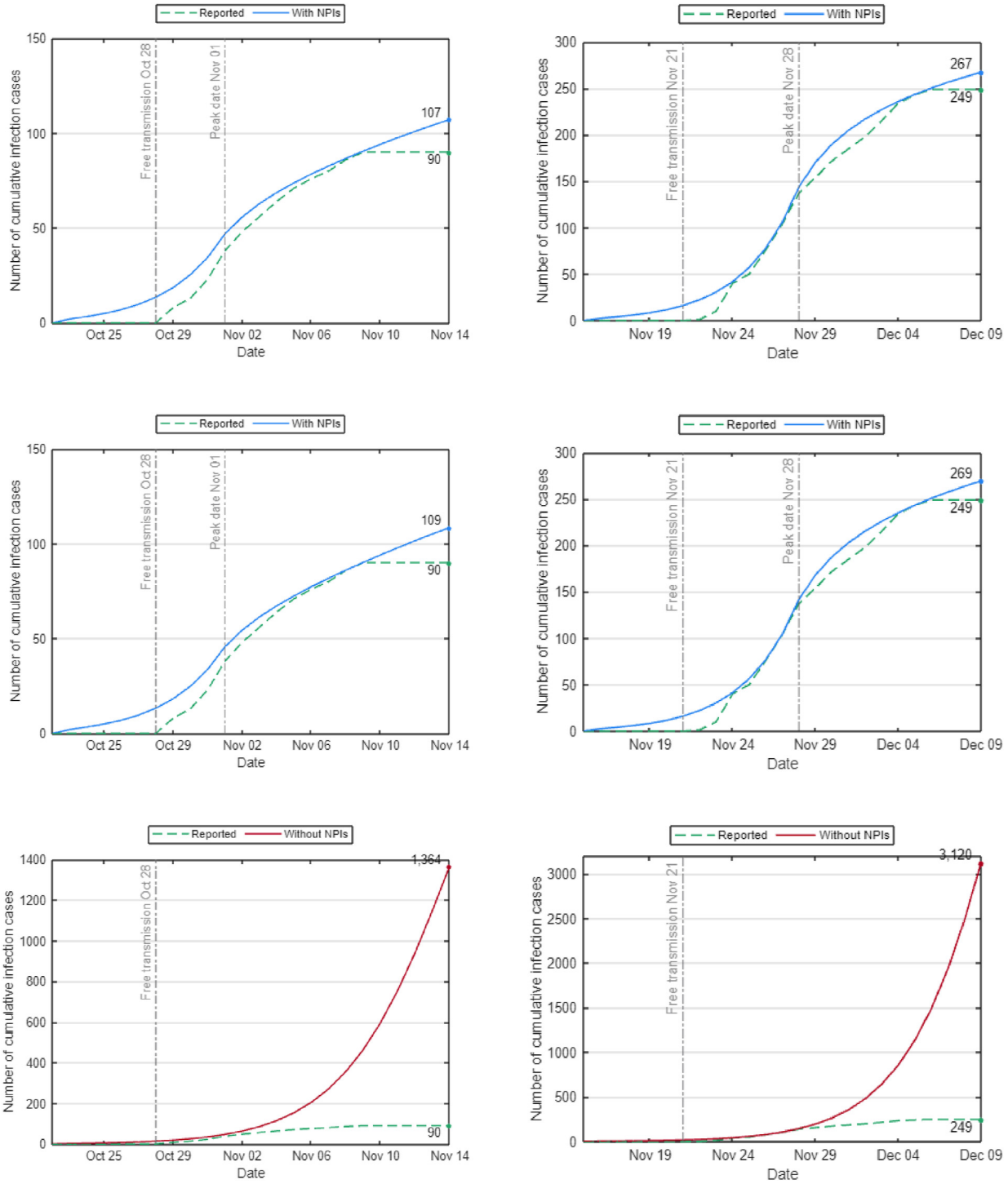

Fig. 2. Numerical simulation for Jinzhou wave 1 (L) and Jinzhou wave 2 (R) in Jinzhou City.

3. Results

3.1. Fitted curves of two epidemics in Jinzhou City

By using the Least Squares Method and parameter values in Supplementary Table 3, the fitted curves for two epidemics in Jinzhou City were performed under three basic assumptions of this study. (i) The awareness delay of two epidemics was set to

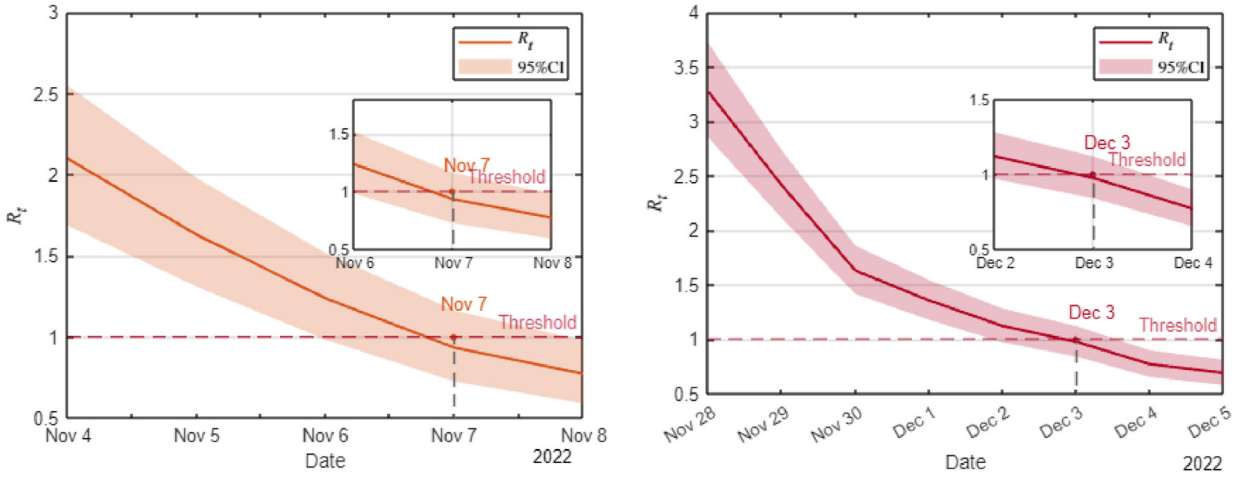

Fig. 3. Changes in Rt for Jinzhou wave 1 (L) and Jinzhou wave 2 (R) in Jinzhou City.

be 7 days. (ii) The values for $\frac{1}{\alpha}$, $\frac{1}{\gamma}$ and ΔT were set to be the same because, by surveillance data from Jinzhou CDC, Omicron BA.5.2 variant and Omicron BA.2.12.1 variant belonged to same lineage when detected. (iii) The control intensity after the implementation of Twenty Measures declined a bit. So, together with the provided data from Jinzhou CDC, the SVEIR model with NPIs for jinzhou wave 1 produced 107 infection cases as of November 14 of 2022 in Fig. 2. If the NPIs were not implemented, the number of infection cases was 1364 as of November 14 of 2022. While, the same simulation for Jinzhou wave 2 with NPIs gave 267 infection cases, the infection scale without NPIs reached 3120 as of December 9 of 2022 in Fig. 2. Alternatively, by the estimated data method, the fitted curves for two epidemics were operated in middle panels of Fig. 2.

3.2. Comparisons of basic reproduction number

By maximum likelihood method, exponential growth rate method, and program R version 4.3.1 combined with infector-infectee pairs of surveillance data, the estimations of $\mathcal{R}_0$ with a 95% confidential interval were performed in Table 2, here, infector-infectee pairs were selected in terms of positive or symptoms. Alternatively, next generation matrix method combined with provided data and estimated data, brought the diversities of estimations in Table 3.

These comparisons showed that the estimations of $\mathcal{R}_0$ by exponential growth rate method were smaller than those by maximum likelihood method, and that the estimations by next generation matrix method were close to those in Table 2. These comparisons also showed that the estimations of $\mathcal{R}_0$ increased from Jinzhou wave 1 before Twenty Measures to Jinzhou

Table 2
Estimations of $\mathcal{R}_0$ by maximum likelihood method and exponential growth rate method.

Sta[a]	Fea[b]	Per[c]	SI[d]	AV[e]	SD[f]	EGR[g]	DT[h]	$\mathcal{R}_0$ (ML)	$\mathcal{R}_0$ (EGR)	NP[i]
1028	S[j]	12	Ga ~(1.87,0.55)	3.43	2.47	0.15	4.62	2.54 (1.58,3.82)	1.72 (0.80,3.22)	46
1028	P[k]	12	Ga ~(1.81,0.52)	3.47	2.55	0.15	4.62	2.55 (1.55,3.84)	1.73 (0.79,3.24)	45
1028	S	7	Ga ~(1.91,0.55)	3.45	2.48	0.15	4.62	2.55 (1.55,3.84)	1.72 (0.79,3.24)	42
1028	P	7	Ga ~(1.90,0.54)	3.54	2.53	0.15	4.62	2.62 (1.63,3.94)	1.74 (0.79,3.30)	41
1121	S	15	Ga ~(2.40,1.01)	2.39	1.54	0.40	1.73	3.26 (2.14,4.73)	2.87 (1.50,5.22)	157
1121	P	15	Ga ~(1.96,0.84)	2.34	1.67	0.40	1.73	3.09 (2.03,4.49)	2.84 (1.50,5.10)	159
1121	S	7	Ga ~(2.50,1.00)	2.50	1.57	0.40	1.73	3.49 (2.29,5.07)	2.95 (1.52,5.45)	124
1121	P	7	Ga ~(2.02,0.83)	2.43	1.70	0.40	1.73	3.24 (2.12,4.70)	2.90 (1.51,5.26)	126

[a] Start time.
[b] Features.
[c] Period.
[d] The serial interval was the time between symptom onsets in an infector-infectee pair, that was, the interval between the onset of symptoms in an infectee and its presumed infector.
[e] Average value of serial interval.
[f] Standard deviation of serial interval.
[g] Exponential growth rate where the exponential growth period was accounted from start date to peak date of an epidemic.
[h] Doubling time.
[i] Number of pairs.
[j] Symptoms.
[k] Positive.

wave 2 after Twenty Measures, which further reflected that the control intensity of local government declined after the implementation of Twenty Measures.

3.3. Estimations of effective reproduction number

By Matlab, the value of $\mathcal{R}_t$ for Jinzhou wave 1 was 2.09 (95%CI: 1.62, 2.64) on November 4, then dropped below 1 on November 7 and remained at a lower value since then. Similarly, the $\mathcal{R}_t$ value of Jinzhou wave 2 was 3.27 (95%CI: 2.78, 3.81) on November 28. It dropped below 1 on December 3 with value 0.97. The study showed that two epidemics led by Omicron variants were effectively controlled.

3.4. Assessments of control strategies

The assessments of three control strategies (awareness delay, peak delay, control intensity) were extensively discussed to explore the impacts of NPIs against the infection scales of two epidemics.

3.4.1. Impacts of awareness delay

Awareness delay is the delay between the date of the first infection and the date of the first confirmation. The awareness delays of two epidemics were set to be 10 days and 14 days respectively in Fig. 4. The results showed that infection scales increased with awareness delay. As of November 14, infection scales of Jinzhou wave 1 increased from baseline to 236, further to 606, respectively. After the implementation of Twenty Measures, by the same scenario discussion, infection scales of Jinzhou wave 2 increased from baseline to 615, further to 1673 as of December 9.

3.4.2. Impacts of peak delay

The peaks of two epidemics were respectively assumed to be extended by 4 days and 8 days in Fig. 5. The results showed that infection scales substantially enhanced with increasing peak delay. Precisely, as of November 14, the infection scale of Jinzhou wave 1 increased from 303 to 743. Similarly, the infection scale of Jinzhou wave 2 varied from 802 to 2065 as of December 9.

3.4.3. Impacts of control intensity

The variations of control intensity against infection scales of two epidemics were investigated. The study showed that infection scale increased with the declining of control intensity in Fig. 6. More precisely, as of November 14, the infection scale of Jinzhou wave 1 increased from 1411 to 3365 as control intensity decreased from 0.8 to 0.6. As of December 9, Jinzhou wave 2 of infection scale varied from 1120 to 6672 under the same control intensity.

The aforementioned investigation and analysis showed that control strategies (awareness delay, peak delay, control intensity) played vital roles in controlling infection scales. Meanwhile, these strategies were effective in declining the infection risk and medical runs, when local government afforded within a moderate financial range.

4. Discussion

4.1. Investigations on variant evolution

If Omicron variant was replaced by EG.5 variant (World Health Drganization, 2023; Sun et al., 2023) during dynamic zero-COVID policy, then, the simulations of two epidemics in Jinzhou City were carried out for effectively monitoring and predicting the variant evolution. Precisely, we kept the initial values and parameter values of two epidemics in Jinzhou City the same as presented in Tables 1 and 3, the awareness delay and control intensity were the same with those in Fig. 2 except for the incubation period and peak delay. This study assumed that the incubation period for EG.5 variant was 1.5 days (Liu et al., 2024), peak delays were extended to 4 days and 8 days respectively. Therefore, the epidemiological characteristics of EG.5 variant were further explored in Fig. 7. The changes of peaks for Jinzhou wave 1 were performed from 12 to 39, further to 308.

Table 3
Estimation of $\mathcal{R}_0$ by next generation matrix method.

DS[a]	Sta[b]	N_0	d_1^{c}	d_2^{d}	β_1^{a} [e]	$\mathcal{R}_0$
Provided data	1028	11,992	10	8	5.04×10^{-3}	4.23
Estimated data	1028	82,942	10	8	7.02×10^{-4}	4.18
Provided data	1121	47,954	13	8	6.83×10^{-4}	4.64
Estimated data	1121	184,677	13	8	1.74×10^{-4}	4.61

[c]Duration of infection rates befor control.
[d]Duration of infection rates after control.
[e]Average infection rates.
[a] Data sources.
[b] Start time.

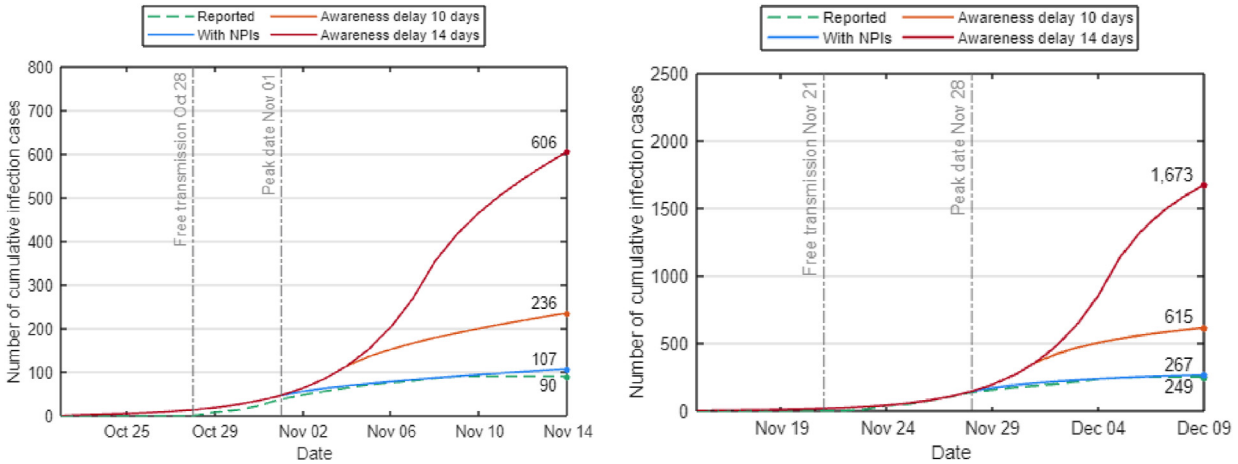

Fig. 4. Infection scales of Jinzhou wave 1 (L) and Jinzhou wave 2 (R) by SVEIR model with awareness delay.

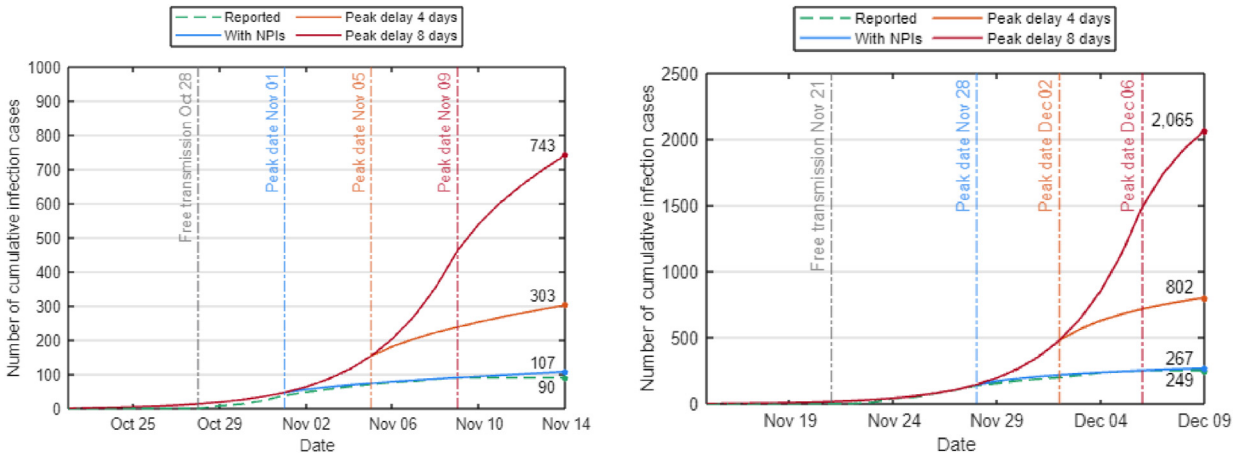

Fig. 5. Infection scales of Jinzhou wave 1 (L) and Jinzhou wave 2 (R) by SVEIR model with peak delay.

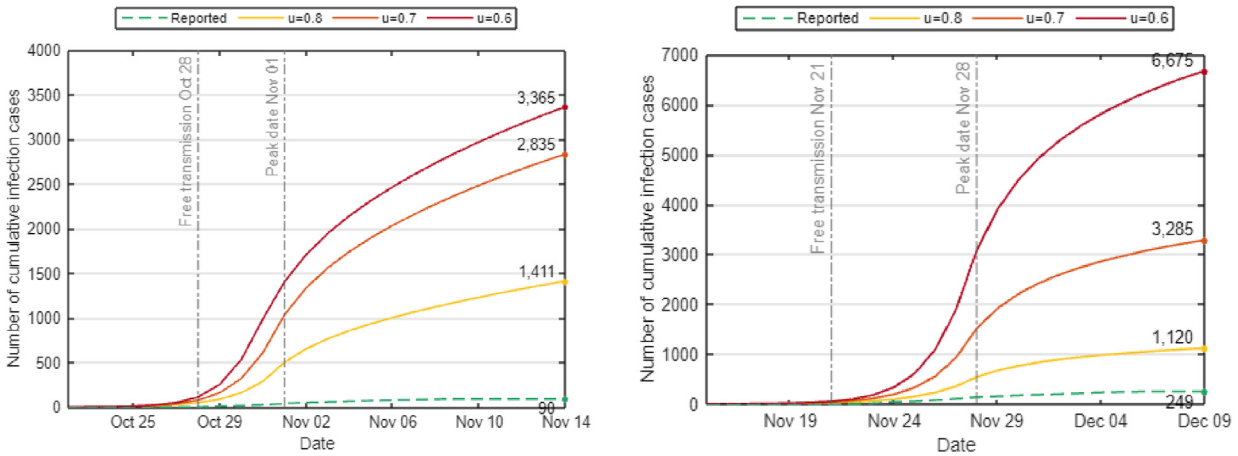

Fig. 6. Infection scales of Jinzhou wave 1 (L) and Jinzhou wave 2 (R) by SVEIR model with control intensity.

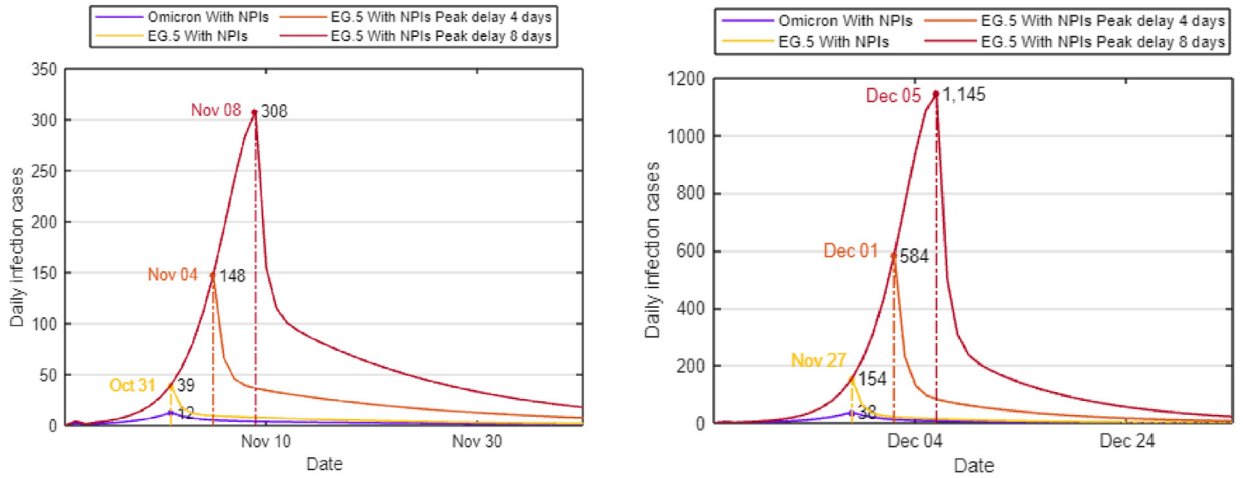

Fig. 7. Daily infection cases led by EG.5 variant against Omicron variant for Jinzhou wave 1 (L) and Jinzhou wave 2 (R) during dynamic zero-COVID policy.

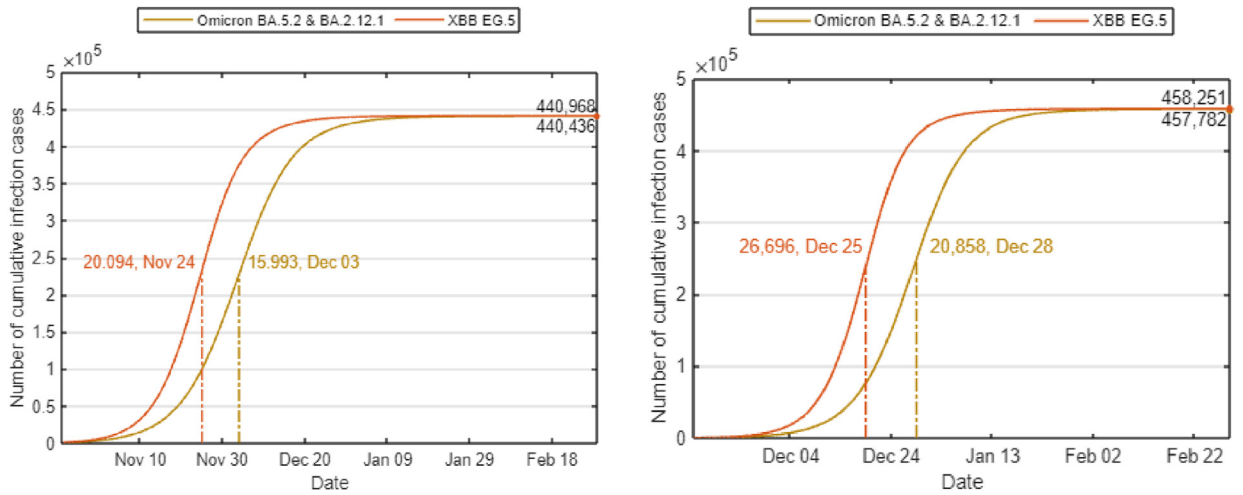

Fig. 8. Daily infection cases and cumulative infection cases of Jinzhou wave 1 (L) and Jinzhou wave 2 (R) without NPIs.

After the implement of Twenty Measures, due to the reduction of control intensity, the daily infection cases of Jinzhou wave 2 with EG.5 variant were extensively increasing with peaks from 38 to 154, further to 1145. As a consequence, the increasing tendency of peaks of infection cases were obvious after Twenty Measures.

If non-pharmaceutical interventions (NPIs) were not implemented, no controls were taken, then, two epidemics in Jinzhou City experienced quite different infection scales. The total population of Jinzhou City involved by two epidemics was taken from the Communiques of the Seventh National Population Census of Jinzhou City, the initial values of the exposed were set in Table 1. Therefore, the number of daily infection cases led by EG.5 variant peaked at 20,094 on November 24. The peak led by Omicron variant was achieved less 4101 infection cases on December 3. The number of cumulative infection cases was around 440,000 for Jinzhou wave 1 as shown on left panel of Fig. 8. While, the daily infection cases and cumulative infection cases of Jinzhou wave 2 were investigated on right panel of Fig. 8. These numerical investigations showed that variant evolution brought increasing infection scales and medical pressures.

4.2. Investigations on public medical requirement

The adequate medical resources were effective and necessary strategies against the prevalence of COVID-19. This study assumed that 0.1% of infection cases were severe or critically ill requiring ICU beds. Based on population data from Communiques of the Seventh National Population Census (Liaoning Provincial Bureau of Statistics, 2021) and the implementation of Twenty Measures, the dates that peaks reached were extensively discussed for Jinzhou City and Liaoning Province. The simulation results showed that if no NPIs were implemented, the requirements of ICU beds were respectively set at 250, 300

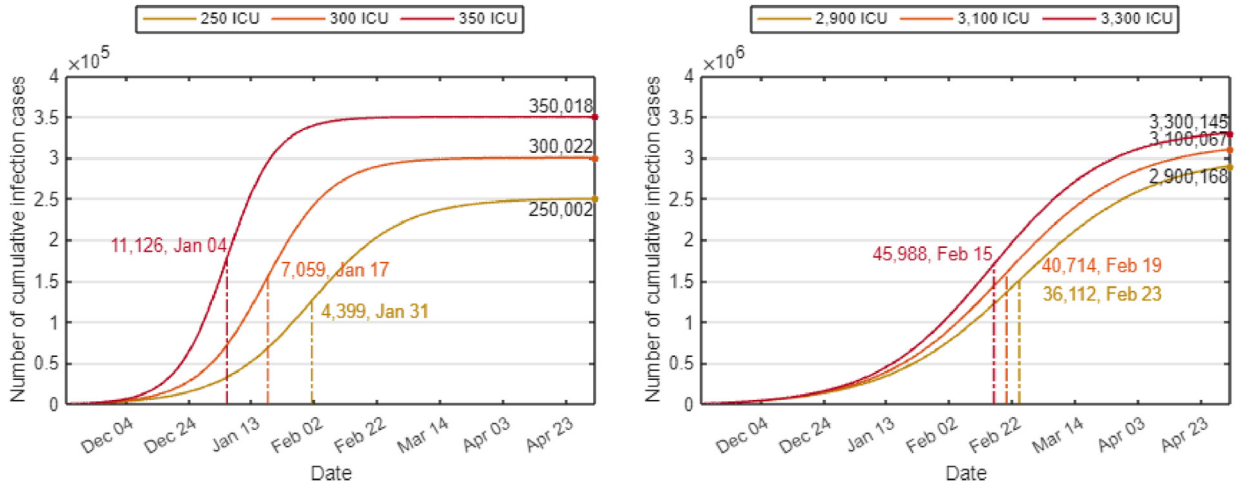

Fig. 9. Simulations of ICU beds requirements for Jinzhou City (L) and Liaoning Province (R).

and 350 for Jinzhou City, then the dates that peaks appeared were January 31, January 17 and January 4 of the year 2023. In other words, the time that reached peaks were respectively shortened 14 days and 27 days compared with baseline scenario (250 ICU beds) as presented on left panel of Fig. 9. By the same argument, the simulation results of Liaoning Province provided the peak on February 23 of the year 2023 with baseline scenario (2900 ICU beds), and also provided the peaks on February 19 and February 15 as presented on right panel of Fig. 9. This showed that the public medical requirement depended on the infection scale and variant evolution, and showed that the routine surveillance of variant evolution was necessary and important.

5. Conclusion

The complex interactions were performed among non-pharmaceutical interventions (NPIs), vaccinations, and hosts during the spread of COVID-19 in mainland China at distinct stages (Liang et al., 2021; Lin et al., 2022). Usually, the NPIs relied on control strategies and routine surveillance for each epidemic of mainland China. Specially, the effective control of Jinzhou two epidemics in 2022 originated from a strong control strategy and early routine surveillance.

In this study, an SVEIR model with control was developed to compare the epidemiological characteristics of two epidemics in Jinzhou City before and after the implementation of Twenty Measures, in which Jinzhou wave 1 was driven by Omicron BA.5.2 variant, and Jinzhou wave 2 by Omicron BA.2.12.1 variant. This study governed maximum likelihood method, exponential growth rate method, and next generation matrix method to estimate basic reproduction number of two epidemics in Jinzhou City, which presented the epidemiological index evolutions with variants. Especially, the implementation of Twenty Measures reflected that both infection scale and basic reproduction number increased with variant, and that the control intensity decreased with variant.

This study also discussed the impacts of control strategies (awareness delay, peak delay and control intensity) for two epidemics in Jinzhou City. The results revealed that the strong control strategy and early routine surveillance were critical for suppression of infection scale of COVID-19 during the implement of a dynamic zero-COVID policy. Meanwhile, the numerical simulations by governing the SVEIR model were carried out for EG.5 variant. The simulation results showed that the peak of infection cases led by EG.5 variant increased up compared with the peak led by Omicron variant in Fig. 7. If no NPIs were implemented, then infection scales and medical pressures caused by variant evolution gradually increased, which were supported by numerical investigations for Jinzhou City in Fig. 8 and Liaoning Province in Fig. 9.

Ethics approval and consent to participate

The ethical approval and individual consents were exempted as the aggregated data were used in this study.

Funding

This study received was supported by the Natural Science Foundation of Fujian Province of China (2021J01621), Consultancy Project by the Chinese Academy of Engineering (2022-JB-06), Project for epidemiological characteristics analysis and clustering epidemics analysis of COVID-19 in Jinzhou City (JZ2024B066).

Author contributors

KJC: analysis, data interpretation, software, drafting and critical review; FYW: data analysis, study design, data interpretation and critical review; ZWW: critical review; XYZ,HJ,YZ,KF: epidemic disposition, epidemiological investigations, data curation.

Data and material availability

The data that supported this article may be available upon reasonable request to the corresponding author.

CRediT authorship contribution statement

Kaijing Chen: Writing – review & editing, Writing – original draft, Visualization, Validation, Software, Resources, Formal analysis, Data curation, Conceptualization. **Fengying Wei:** Writing – review & editing, Supervision, Project administration, Methodology, Investigation, Formal analysis. **Xinyan Zhang:** Writing – review & editing, Investigation, Data curation. **Hao Jin:** Writing – review & editing, Investigation, Data curation. **Zuwen Wang:** Writing – review & editing, Investigation, Data curation, Conceptualization. **Yue Zuo:** Writing – review & editing, Investigation, Data curation. **Kai Fan:** Writing – review & editing, Investigation, Data curation.

Declaration of competing interest

The authors declare that they have no known competing financial interests or personal relationships that could have appeared to influence the work reported in this paper.

Acknowledgements

FYW was supported by Natural Science Foundation of Fujian Province of China (2021J01621), and Consultancy Project by the Chinese Academy of Engineering (2022-JB-06).

Appendix A. Supplementary data

Supplementary data to this article can be found online at https://doi.org/10.1016/j.idm.2024.03.005.

References

Chen, T., Rui, J., Wang, Q., Zhao, Z., Cui, J., & Yin, L. (2020). A mathematical model for simulating the phase-based transmissibility of a novel coronavirus. *Infectious Diseases of Poverty, 9*, 1–8. https://doi.org/10.1186/s40249-020-00640-3

Chen, L., & Wei, F. (2020). Study on a susceptible-Exposed-Infected-Recovered model with nonlinear incidence rate. *Advances in Difference Equations, 2020*(206), 1–21. https://doi.org/10.1186/s13662-020-02662-5

Chowell, G., & Nishiura, H. (2009). *The effective reproduction number as a prelude to statistical estimation of time-dependent epidemic trends. mathematical and statistical estimation approaches in epidemiology. Mathematical and Statistical Estimation Approaches in Epidemiology* (pp. 103–121).

Cori, A., Ferguson, N. M., Fraser, C., & Cauchemez, S. (2013). A New framework and software to estimate time-varying reproduction numbers during epidemics. *American Journal of Epidemiology, 178*, 1505–1512. https://doi.org/10.1093/aje/kwt133

Forsberg White, L., & Pagano, M. (2008). A likelihood-based method for real-time estimation of the serial interval and reproductive number of an epidemic. *Statistics in Medicine, 27*, 2999–3016. https://doi.org/10.1002/sim.3136

Guo, Y., Wu, S., Ye, W., Zhao, Z., Li, K., Guo, X., et al. (2022). Impact of public health and social measures on contact dynamics during a SARS-CoV-2 Omicron variant outbreak in Quanzhou, China, March to April. *International Journal of Infectious Disease, 131*, 46–49. https://doi.org/10.1016/j.ijid.2023.03.025

Guo, Y., Ye, W., Zhao, Z., Guo, X., Song, W., Su, Y., et al. (2023). Simulating potential outbreaks of delta and Omicron variants based on contact-tracing data: A modelling study in fujian Province, China. *Infectious Disease Modelling, 8*, 270–281. https://doi.org/10.1016/j.idm.2023.02.002

Hamou, A. A., Rasul, R. R. Q., Hammouch, Z., & Özdemir, N. (2022). Analysis and dynamics of a mathematical model to predict unreported cases of COVID-19 epidemic in Morocco. *Computational and Applied Mathematics, 41*, 1–33. https://doi.org/10.1007/s40314-022-01990-4

He, D., Cowling, B. J., Ali, S. T., & Stone, L. (2023). Rapid global spread of variants of concern of SARS-CoV-2. *IJID Regions, 7*, 63–65. https://doi.org/10.1016/j.ijregi.2022.12.005

He, S., Yang, J., He, M., et al. (2021). The risk of future waves of COVID-19: Modeling and data analysis. *Mathematical Biosciences and Engineering, 18*(5), 5409–5426. https://doi.org/10.3934/mbe.2021274

Hellewell, J., Abbott, S., Gimma, A., Bosse, N. I., Jarvis, C. I., Russell, T. W., et al. (2020). Feasibility of controlling COVID-19 outbreaks by isolation of cases and contacts. *Lancet Global Health, 8*, e488–e496. https://doi.org/10.1016/S2214-109X(20)30074-7

Huang, S., Wei, F., Peng, Z., et al. (2020). Assessment method of coronavirus disease 2019 outbreaks under normal prevention and control. *Disease Surveillance, 8*, 679–686.

Jinzhou Bureau of Statistics. (2023). Communiques of the Seventh national population Census of jinzhou city. http://tjj.jz.gov.cn/info/1058/3395.htm.

Lan, X., Chen, G., Zhou, R., Zheng, K., Cai, S., Wei, F., Jin, Z., & Mao, X. (2023a). Studying a stochastic COVID-19 model with age group and social activation. *Mathematical Biosciences. Under Review*.

Lan, X., Chen, G., Zhou, R., Zheng, K., Cai, S., Wei, F., Jin, Z., & Mao, X. (2023b). Studying a COVID-19 model with age group and social activation in Fuzhou large wave, Infectious Disease Modelling. *Under Review*.

Lan, X., Chen, G., Zhou, R., Zheng, K., Cai, S., Wei, F., Jin, Z., & Mao, X. (2023c). Studying an age heterogeneous SEIHR model with social activations. *Journal of Mathematical Biology Under Review*.

Li, D., Wei, F., & Mao, X. (2022). Stationary distribution and density function of a stochastic SVIR epidemic model. *Journal of the Franklin Institute, 359*, 9422–9449. https://doi.org/10.1016/j.jfranklin.2022.09.026

Li, T., & Xiao, Y. (2023). Optimal strategies for coordinating infection control and socio-economic activities. *Mathematics and Computers in Simulation, 207*, 533–555. https://doi.org/10.1016/j.matcom.2023.01.017
Liang, W., Yao, J., Wu, J., Liu, X., Liu, J., Zhou, L., et al. (2021). Experience and thinking on the normalization stage of prevention and control of COVID-19 in China. *National Medical Journal of China, 101*(10), 695–699. https://doi.org/10.3760/cma.j.cn112137-20210104-00008
Liaoning Provincial Bureau of Statistics. (2021). Communiques of the Seventh national population Census of liaoning Province. https://tjj.ln.gov.cn/tjj/tjsj/tjgb/rkpcgb/20231108180300877797/index.shtml.
Lin, Q., Musa, S. S., Zhao, S., & He, D. (2020). Modeling the 2014-2015 ebola virus disease outbreaks in Sierra Leone, Guinea, and Liberia with effect of high- and low-risk susceptible individuals. *Bulletin of Mathematical Biology, 82*, 1–23. https://doi.org/10.1007/s11538-020-00779-y
Liu, J., Liu, M., & Liang, W. (2022). The dynamic COVID-zero strategy in China. *China CDC Weekly, 4*(4), 74–75. https://doi.org/10.46234/ccdcw2022.015
Liu, C., Lu, J., Li, P., Feng, S., Guo, Y., Li, K., et al. (2023). A comparative study on epidemiological characteristics, transmissibility, and pathogenicity of three COVID-19 outbreaks caused by different variants. *International Journal Infectious Disease, 134*, 78–87. https://doi.org/10.1016/j.ijid.2023.01.039
Liu, H., Xu, X., Deng, X., Hu, Z., Sun, R., Zou, J., et al. (2024). Counterfactual analysis of the 2023 Omicron XBB wave in China. *Infectious Disease Modelling, 9*, 195–203. https://doi.org/10.1016/j.idm.2023.12.006
Lovell-Read, F. A., Shen, S., & Thompson, R. N. (2022). Estimating local outbreak risks and the effects of non-pharmaceutical interventions in age-structured populations: SARS-CoV-2 as a case study. *Journal of Theoretical Biology, 535*, Article 110983. https://doi.org/10.1016/j.jtbi.2021.110983
Lu, R., & Wei, F. (2019). Persistence and extinction for an age-structured stochastic SVIR epidemic model with generalized nonlinear incidence rate. *Physica A: Statistical Mechanics and Its Applications, 513*, 572–587. https://doi.org/10.1016/j.physa.2018.09.016
Niu, Y., & Xu, F. (2020). Deciphering the power of isolation in controlling COVID-19 outbreaks. *Lancet Global Health, 8*, e452–e453. https://doi.org/10.1016/S2214-109X(20)30085-1
Shen, M., Zu, J., Fairley, C. K., Pagán, J. A., An, L., Du, Z., et al. (2021). Projected COVID-19 epidemic in the United States in the context of the effectiveness of a potential vaccine and implications for social distancing and face mask use. *Vaccine, 39*, 2295–2302. https://doi.org/10.1016/j.vaccine.2021.02.056
Song, H., Wang, R., Liu, S., Jin, Z., & He, D. (2022). Global stability and optimal control for a COVID-19 model with vaccination and isolation delays. *Results in Physics, 42*, Article 106011. https://doi.org/10.1016/j.rinp.2022.106011
Sun, Y., Wang, M., Wei, F., Huang, S., & Xu, J. (2023). COVID's future: Viral multi-lineage evolution and the dynamics of small epidemic waves without seasonality in COVID-19. *Journal of Biosafety and Biosecurity, 5*, 96–99. https://doi.org/10.1016/j.jobb.2023.07.003
Tang, B., Wang, X., Li, Q., Bragazzi, N. L., Tang, S., Xiao, Y., et al. (2020). Estimation of the transmission risk of the 2019-nCoV and its implication for public health interventions. *Journal of Clinical Medicine, 9*, 462. https://doi.org/10.3390/jcm9020462
The State Council joint prevention and control mechanism against COVID-19. (2022). Ten measures. https://www.gov.cn/xinwen/2022-11/11/content.5730443.htm.
The State Council joint prevention and control mechanism against COVID-19. (2022a). Twenty measures. https://www.gov.cn/xinwen/2022-11/11/content5726144.htm.
Van den Driessche, P. (2017). Reproduction numbers of infectious disease models. *Infectious Disease Modelling, 2*, 288–303. https://doi.org/10.1016/j.idm.2017.06.002
Van den Driessche, P., & Watmough, J. (2002). Reproduction numbers and sub-threshold endemic equilibria for compartmental models of disease transmission. *Mathematics Biosciences, 180*, 29–48. https://doi.org/10.1016/S0025-5564(02)00108-6
Wallinga, J., & Lipsitch, M. (2007). How generation intervals shape the relationship between growth rates and reproductive numbers. *Proceedings of the Royal Society B: Biological Sciences, 274*, 599–604. https://doi.org/10.1098/rspb.2006.3754
Wei, X., Li, M., Pei, X., Liu, Z., & Zhang, J. (2023). Assessing the effectiveness of the intervention measures of COVID-19 in China based on dynamical method. *Infectious Disease Modelling, 8*, 159–171. https://doi.org/10.1016/j.idm.2022.12.007
Wei, F., & Xue, R. (2020). Stability and extinction of SEIR epidemic models with generalized nonlinear incidence. *Mathematics and Computers in Simulation, 170*, 1–15. https://doi.org/10.1016/j.matcom.2018.09.029
Wei, F., Zhou, R., Jin, Z., Huang, S., Peng, Z., Wang, J., et al. (2023). COVID-19 transmission driven by age-group mathematical model in Shijiazhuang City of China. *Infectious Disease Modelling, 8*, 1050–1062. https://doi.org/10.1016/j.idm.2023.08.004
World Health Drganization. (2023). Tracking SARS-CoV-2 variant. https://www.who.int/en/activities/tracking-SARS-CoV-2-variants/.
Xiong, S., Cai, S., Zhou, R., Wei, F., Chen, G., & Zheng, K. (2024). Studying an SVEIR mathmatical model withvarying variant. *Mathematical Biosciences and Engineering*. submitted for publication.
Yu, B., Li, Q., Chen, J., & He, D. (2023). The impact of COVID-19 vaccination campaign in Hong Kong SAR China and Singapore. *Infectious Diseasse Modelling, 8*, 101–106. https://doi.org/10.1016/j.idm.2022.12.004
Zhao, S., Wang, K., Chong, M. K. C., Musa, S. S., He, M., Han, L., et al. (2022). The non-pharmaceutical interventions may affect the advantage in transmission of mutated variants during epidemics: A conceptual model for COVID-19. *Journal of Theoretical Biology, 542*, Article 111105. https://doi.org/10.1016/j.jtbi.2022.111105
Zou, Z., Fairley, C. K., Shen, M., Scott, N., Xu, X., Li, Z., et al. (2022). Critical timing and extent of public health interventions to control outbreaks dominated by SARS-CoV-2 variants in Australia: A mathematical modelling study. *International Journal of Infectious Disease, 115*, 154–165. https://doi.org/10.1016/j.ijid.2021.11.024